

Bar breakage detection on Squirrel Cage Induction Motors via Transient Motor Current Signal Analysis based on the Wavelet Transform. A Review.

Joan Pons-Llinares¹, Vicente Climente-Alarcón¹, Rubén Puche-Panadero¹ and Jose A. Antonino-Daviu¹

¹ Departamento de Ingeniería Eléctrica
Universidad Politécnica de Valencia

Campus de Vera – Valencia, 46022 Valencia (España)

Tel.:+34 963877007, fax:+34 963879009, e-mail: jpons@die.upv.es, viclial@csa.upv.es, rupucpa@die.upv.es,
joanda@die.upv.es

Abstract. The use of the Wavelet Transform for the diagnosis of electrical machines has been widely studied. The present paper explains the main four general approaches in which the Startup Current (SC) of an Squirrel Cage Induction Motor is analyzed using the Wavelet Transform, in order to detect bar breakages: to generate the scalogram of the SC, to calculate the wavelet ridges, to calculate the DWT coefficients or to decompose the SC on a sum of an approximation and detail signals. Examples of those four main approaches are given and the specific solutions proposed by their authors are explained. Through the revision, the Wavelet Transform has proved to be an excellent mathematical tool for the detection of broken bars.

Kew words: TMCSA, startup current, fault diagnosis, induction machines, wavelet transform, broken bars.

1. Introduction

The Startup Current (SC) of a squirrel cage induction motor (SCIM) with a broken bar, does not differ at first sight from the startup current of a healthy one. However, the current under the faulty condition contains harmonics which are characteristic of the fault. More precisely, the breakage of a rotor bar produces a perturbation on the air-gap field inducing characteristic frequencies in the stator current. Those frequencies, dependant on the slip s and on the mains frequency f_{net} , are given by (1) and (2) [1]:

$$f_{bb} = [1 \pm 2ks] f_{net} \quad (1)$$

$$f_{bb} = \left[\frac{k}{p} (1-s) \pm s \right] f_{net} \quad (2)$$

where p is the number of pole pairs. In (1) k is any positive integer and in (2) $k/p = 1, 3, 5, \dots$

Among this set of harmonics, the most important are the so-called Lower Sideband Harmonic (LSH) and the Upper Sideband Harmonic (USH). Their frequencies are given by (1) when $k = 1$:

$$f_{LSH} = f_{net} |1 - 2s| \quad (3)$$

$$f_{USH} = f_{net} (1 + 2s) \quad (4)$$

In (3), we have considered the absolute value in order to obtain a positive value of the LSH frequency.

At steady state, the slip is low, and the frequencies of the Sideband Harmonics (SH), given by (3) and (4), take

values very close and equally separated from f_{net} . If the SCIM has a broken bar, the power spectrum of the steady state stator current will show two peaks on both sides around f_{net} , caused by the presence of the SH. The detection of those two peaks, using the Fast Fourier Transform (FFT), enables the bar breakage diagnosis. This is the classic diagnostic method ([2] – [4]).

The classic method has the following drawbacks:

- The use of a compact support window when applying the FFT produces spectral leakage: when picturing the power spectrum, the energy of the fundamental component (FC) is not well localized on f_{net} , spreading over the surrounding frequencies. This effect can hide the presence of the SH [5], [6].
- The bar breakage is not detected if the machine works at a very low slip (this is the case of light – loaded machines or unloaded machines and it could be the case of some high power motors) [7]. In this case, the SH peaks are very close to the f_{net} peak and have no chance of escaping from the spectral leakage.
- Moreover, if the machine is tested light – loaded or unloaded, the amplitudes of the SH, which depend on the value of the rotor currents, are very small.
- A load variation during the test can invalidate it: the slip varies too, which implies a change on the SH frequencies. This can produce a smearing effect on the current power spectrum, hiding the SH [7].
- Also, the following phenomena may produce in steady – state harmonics similar to the SH: ball bearing defects, voltage fluctuations, load oscillations [8], speed reducing devices such as gearboxes [9] and motors with “spidered” rotor structures that have the same number of legs and poles [10]. This can cause an erroneous diagnostic.
- The method has serious difficulties when diagnosing the condition of the outer cage of double – cage machines [11].

Some recent steady state methods have solved some of these disadvantages ([1], [12] – [14]).

A completely different approach, the so-called Transient Motor Current Signal Analysis (TMCSA), analyzes the stator current during a transient, usually the startup. The analysis consists of applying a certain mathematical tool to the transient stator current, usually a signal analysis technique able to characterize non-

stationary signals such as the Wavelet Transform (WT). The result of the analysis must be sensitive to the presence of the SH. This sensitiveness allows the detection of a bar breakage.

An important advantage of the TMCSA methods is that, regardless of the load conditions, the amplitudes of the SH during the startup, reach values several times higher than those in steady state [15]. As a result of that, the proofs of the bar breakage are much more evident. For some TMCSA methods, the diagnosis of light – loaded or unloaded machines is no longer a problem.

Moreover, when the slip changes during the startup, the frequencies given by (3) and (4) change, leading to a unique time-frequency evolution pattern of the LSH and USH harmonics. Supposing a linear evolution of the slip during the startup and taking $f_{net} = 50$ Hz we obtain:

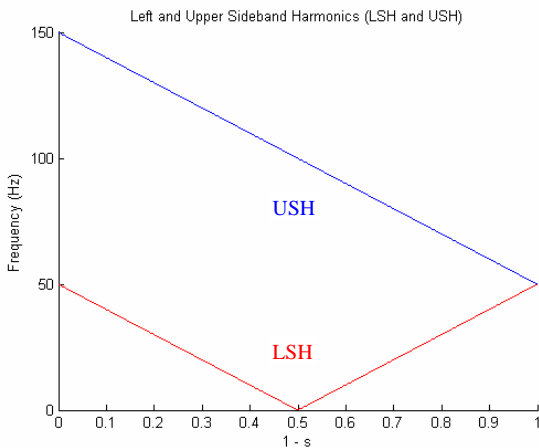


Fig. 1. Time - frequency evolution of the LSH and USH during the startup, supposing a linear evolution of the slip and considering $f_{net} = 50$ Hz .

In other words, the fault produces a distinctive pattern on the startup current recognizable, in the time-frequency plane, like a person signature. The problem is to make it visible in order to detect the fault. This is the objective of some TMCSA methods, achieved by representing in the time-frequency plane the time evolution of the startup current harmonics. If a fault is present, not only the fault related harmonics will be identified, but also their unique time – frequency evolution pattern. This feature greatly increases its reliability, helping to discard non-fault related harmonics like those generated by periodic loads or voltage unbalances.

TMCSA has other advantages: it is non-invasive, it requires only the measurement of a single phase current, it can discriminate between multiple types of failures occurring simultaneously, and it can be performed online, without perturbing the installation operation conditions.

The difference between TMCSA methods is the mathematical tool used to analyze the transient stator current. This leads to advantages and drawbacks. Most TMCSA methods are based on the WT, which has proved to give very good results. On the present paper, TMCSA methods based on the WT are reviewed, specially the ones that analyze the SC.

2. Bar breakage detection via WT.

The present section summarizes the main concepts around the Wavelet Transform (WT), describing how it can be used to detect broken bars on SCIM. The different general approaches for the bar breakage detection based on the WT explained in this section, will help to understand the more specific approaches summarized in the next section. In spite of the difference between those more specific approaches, and the difference between their results, they are all based on some main concepts. The mathematical rigor has been put aside for the benefit of a more intuitive and quickly understanding. The beautiful mathematical construction of the Wavelet Transform and its properties can be found in [16] and [17].

A. Concept of wavelet and wavelet family.

The first concept that must be introduced is the concept of wavelet. A wavelet ψ is what Mallat calls a time-frequency atom; that is, a function well concentrated in time and in frequency. In other words, the time instants for which the wavelet takes significant values, will be concentrated on a certain time region (usually around the origin). Outside that region (called the effective time support), the wavelet function is nearly zero. On the other hand, the frequencies for which the Fourier Transform (FT) of the wavelet $\hat{\psi}$ takes significant values, will be concentrated on a certain frequency band. Outside that band, the function $\hat{\psi}$ is nearly zero. The time – frequency concentration is the main requirement for a function to be a wavelet.

Let us see an example. The following function, known as the Mexican Hat:

$$\psi(t) = \frac{2}{\sqrt{3}\sqrt{\pi}}(1-t^2)\exp\left(-\frac{t^2}{2}\right) \quad (5)$$

is a wavelet. In Fig. 2 left, we can see the Mexican Hat, which is nearly zero for $|t| > 5$. That is, is well concentrated in time. In Fig. 2 right, we can see the FT of the Mexican Hat, which is nearly zero for $|\omega| > 5$. That is, is well concentrated in frequency.

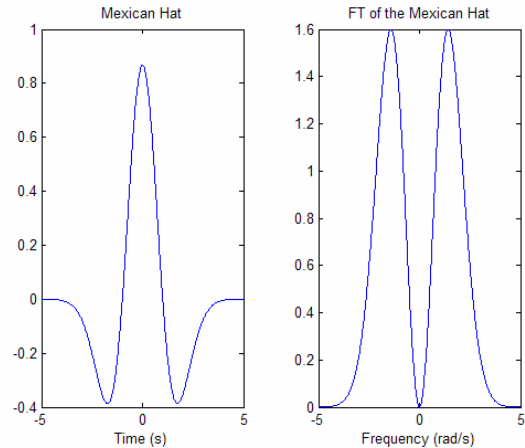


Fig. 2. Mexican Hat (left) and its Fourier Transform (right).

Scaling the wavelet by a (called the scaling parameter) and translating it by b (called the time parameter) we obtain a wavelet family:

$$\psi^{a,b}(t) = \frac{1}{\sqrt{|a|}} \psi\left(\frac{t-b}{a}\right) \quad (6)$$

The original wavelet ψ is known as the mother wavelet and the wavelets $\psi^{a,b}$ obtained using (6) are called the sons.

Let us continue with the Mexican Hat example. In Fig. 3, the mother wavelet has been represented in each plot (in blue) accompanied by one of his sons (in red). The values of a and b used in each case are indicated on top of each plot.

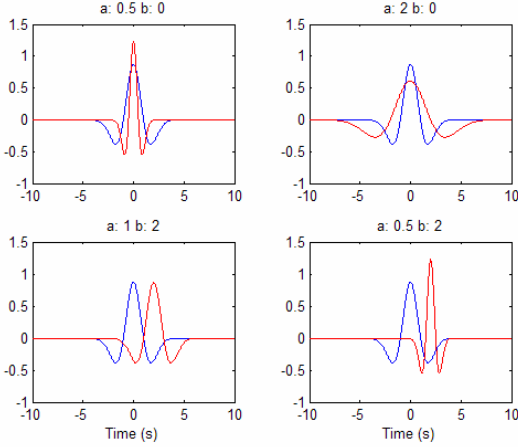


Fig. 3. Each plot represents the mother wavelet (in blue) and one of his sons (in red). The values of the scaling and time parameter used to create the son are indicated on top of the plot.

The mother wavelet energy is concentrated in time around $t=0$. On the other hand, its energy is concentrated in frequency around $\omega = \eta$ (where η is a parameter called the center frequency of the wavelet). We can say that the energy of the mother wavelet is concentrated in the time – frequency plane around the point $[0, \eta]$.

Each member of the wavelet family is also a time – frequency atom: a wavelet son is well concentrated in time and in frequency. The point of the time – frequency plane around which the energy of the wavelet son is concentrated depends on a and b . The energy of a wavelet son $\psi^{a,b}$ is well concentrated in time around $t=b$; and is well concentrated in frequency around $\omega = \eta/a$. This is logic, a son generated taking $a > 1$, reproduces the form of the mother wavelet “more slowly”. Therefore, its energy will be concentrated in frequency around a smaller value: $\omega = \eta/a < \eta$. A son generated taking $a < 1$, reproduces the form of the mother wavelet “more quickly”. Therefore, its energy will be concentrated in frequency around a higher value: $\omega = \eta/a > \eta$.

Concluding, the energy of a wavelet son $\psi^{a,b}$ is concentrated in the time – frequency plane around the point $[b, \eta/a]$.

B. Continuous Wavelet Transform (CWT).

Imagine we want to analyze a signal f which is a sum of different components whose frequencies change in time (that is, a non – stationary signal). More specifically, we want to know how many components it has and how their frequencies vary. This is exactly our problem when diagnosing a SCIM via the analysis of a SC.

In order to diagnose a SCIM, we have measured a SC. At first sight, we can not confirm if the SC is composed only by the FC (whose frequency is constant and equal to f_{net}), or it has also the bar breakage related components (that is, the SH, whose frequencies evolve in the time – frequency plane as shown in Fig. 1). How can we detect the presence of the SH?

The Wavelet Transform (WT) of the signal f at time b and frequency η/a can tell us if the signal f has a component whose frequency takes a value of η/a at time b . The WT of the signal f at time b and frequency η/a is formally defined as the following integral:

$$(T^{wav} f)\left(b, \frac{\eta}{a}\right) = \int_{-\infty}^{+\infty} f(t) \psi^{a,b*}(t) dt \quad (6)$$

where $\psi^{a,b*}$ is the conjugate of $\psi^{a,b}$. Remember that, the energy of a wavelet son $\psi^{a,b}$ is concentrated in the time – frequency plane around the point $[b, \eta/a]$.

The modulus square of the WT, that is $\left|(T^{wav} f)\left(b, \frac{\eta}{a}\right)\right|^2$, is a measure of the energy density of the signal f around the point $[b, \eta/a]$ of the time – frequency plane. If $\left|(T^{wav} f)\left(b, \frac{\eta}{a}\right)\right|^2$ is a high value, it means that f has a component with frequency η/a at time b . Calculating $\left|(T^{wav} f)\left(b, \frac{\eta}{a}\right)\right|^2$ for a wide set of points $[b, \eta/a]$ of the time – frequency plane, and colouring each point depending on the result, we obtain the time evolution of the frequencies of the signal components. This plot is called a scalogram.

In the case of the SC of a SCIM with a broken bar, the scalogram should resemble Fig. 1 plus a constant value equal to f_{net} caused by the FC. If the SCIM is healthy, only the constant value should appear on the scalogram.

The main problem of this approach is that consumes a high computational time. This is due to the fact that the WT has to be calculated for a lot of points of the time – frequency plane in order to obtain a scalogram with enough detail.

Instead of generating the whole scalogram, we can calculate the wavelet ridges: local maxima of the scalogram. The ideal result when applying the ridges algorithm is a 2D plot with traces representing the instantaneous frequency of the signal components.

This version of the WT is known as the Continuous Wavelet Transform (CWT). When f is a discrete signal (almost always), (6) is slightly modified in order to

enable the computation of the integral.

C. Discrete Wavelet Transform (DWT).

A signal f can be decomposed, using the WT, in the so-called approximation signal a_n and the n detail signals d_n, \dots, d_1 . That is:

$$f = a_n + d_n + \dots + d_1 \quad (7)$$

Each signal covers a frequency band that depends on the sampling rate f_s used for capturing f and on the decomposition level n chosen ($n \in \mathbb{N}$). The detail signal d_j contains the components of f whose frequencies are included in the frequency band $[2^{-(j+1)} f_s, 2^{-j} f_s]$. The approximation signal a_n includes the low frequency components of the signal, belonging to the interval $[0, 2^{-(n+1)} f_s]$.

The order j detail signal (d_j) is a weighted sum of the wavelet sons $\psi^{2^j, k2^j}$, where $k \in \mathbb{Z}$. The weighting coefficients are the WT of the analyzed signal $(T^{wav} f)(k2^j, \eta/2^j)$ calculated at the scale $a = 2^j$ and time instants $b = k2^j$. In other words:

$$d_j = \sum_k [(T^{wav} f)(k2^j, \eta/2^j)] \psi^{2^j, k2^j} \quad (8)$$

The approximation signal is calculated using the so-called scaling function (which will not be defined for space reasons): it is a weighted sum of translated and scaled versions of the scaling function.

The set of the weighting coefficients $(T^{wav} f)(k2^j, \eta/2^j)$ (calculated for the scales $a = 2^j$ with $j = 1, \dots, n$, and time instants $b = k2^j$ with $k \in \mathbb{Z}$), and the weighting coefficients used to calculate the approximation signal, is called the DWT of the signal f . In the case of a discrete signal f , the DWT can be very quickly calculated using Mallat algorithm, which is its main advantage.

Let's see an example. In order to diagnose a SCIM, if the SC has been sampled with $f_s = 5000$ Hz, we can calculate the wavelet coefficients at the scale $j = 7$ such as $[2^{-(j+1)} f_s, 2^{-j} f_s] \in [19, 39]$. If the wavelet coefficients at that scale:

$$(T^{wav} f)(k2^j, \eta/2^j) \quad k \in \mathbb{Z} \quad (9)$$

get high values, it means that the SC has a component on the associated frequency band $[19, 39]$. This can mean the presence of the LSH, related to the bar breakage.

The DWT can also be used to calculate the approximation and detail signals. If the signals covering the frequency band $[0, 50]$ have significant amplitudes and fluctuations, this can mean the presence of the LSH.

3. Examples of specific solutions proposed.

The diagnosis methods reviewed in the present section, apply the WT to the SC of the SCIM being diagnosed in order to detect a bar breakage. They have been classified depending on the version of the WT used: the Discrete Wavelet Transform (DWT) or the Continuous Wavelet Transform (CWT).

A. CWT

Supangat et al. [18] propose to analyze the SC via the generation of the scalogram using a DB8 wavelet. The presence of the SH produces some differences between the scalogram of the SC belonging to a SCIM with a broken bar and the scalogram of a healthy SC. However, the FC overshadows those differences. In order to eliminate that undesirable effect, they propose to analyze the envelope of the SC, which does not depend on the FC. The effect of the SH presence was highlighted, obtaining a much more objective diagnosis criterion.

Zhengping Zhang et al. [19] base their diagnosis method on calculating the wavelet ridges of the SC. If the SCIM analyzed is healthy, in the $[0, f_{net}]$ frequency band there is only an important component (apart from the Principal Slot Harmonics): the FC which has a constant frequency equal to f_{net} . Therefore, the representation of the wavelet ridges of the SC on a 2D plot as a function of time, shows only a constant frequency equal to f_{net} . If the SCIM analyzed has a broken bar, on the $[0, f_{net}]$ frequency range appears a new component: the LSH, whose frequency varies during the startup as shown in Fig. 1. Therefore, wavelet ridges may be able to reflect the LSH time – frequency evolution pattern, apart from the constant frequency equal to f_{net} . In [19], only the last part of the startup has been analyzed: only the last part of the LSH time – frequency evolution pattern appears on the 2D plot. Moreover, between the two frequencies present on the frequency range analyzed (FC frequency and LSH frequency), only one is reflected on the 2D plot at a time.

Briz et al. [20], instead of using an already existing wavelet (a Gabor Wavelet, a Daubechies Wavelet, etc.), design a specific wavelet resembling the shape of the LSH. Using this wavelet, they calculate the CWT modulus of the SC for a set of values of the scaling a and time b parameters. The result is represented on a coloured 2D plot. When the SCIM analyzed has a broken bar, the plot shows very high values at a certain scale and particularly at a certain time interval. Finally, the method proposes plotting the CWT modulus as a function of a , for a time instant belonging to the mentioned time interval. In this last plot, the highest values of the CWT modulus are viewed as a peak, produced by the presence of the LSH, which enables the detection of the broken bar.

B. DWT

In [15] and [21], the DWT was used to decompose the

SC in an approximation signal and n details (n is the decomposition level), each one containing the harmonics of a different frequency band. Figure 4 reproduces some of the results of [15] (Fig. 4 and 5 of [15]). It shows the approximation signal of a healthy and a rotor broken bar machine driving a pure inertia load (startup of 2 seconds), using a DB44 wavelet, $n = 6$, $f_s = 5000$ samples/second. The approximation signal contains the harmonics with frequencies in the interval $[0, 2^{-(n+1)}]f_s \square [0, 39]Hz$, that is, almost the whole band where the LSH is present $[0, 50]Hz$. In other words, the approximation signal contains almost the whole LSH. When a machine has a broken rotor bar, the presence of the LSH increases the amplitude of the approximation signal, enabling the fault detection and diagnosis. On the other hand, taking into account that in that frequency range the LSH is the only significant component (apart from the electromagnetic transient and the beginning of some Principal Slot Harmonics), obtaining that approximation signal means to extract the LSH from the SC (if there is any LSH). In [15], a parameter to quantify the fault severity has been introduced. It is defined as 10 times the logarithm of the quotient between the SC energy and the approximation signal energy.

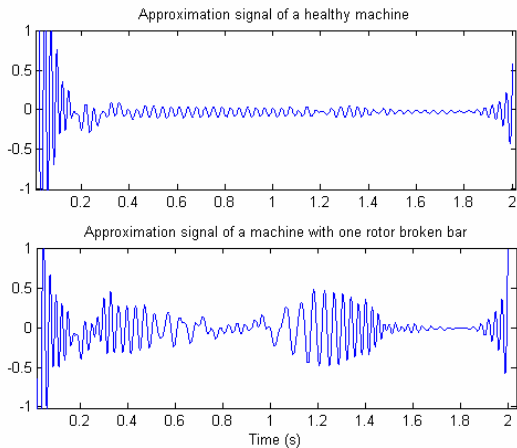


Fig. 4 Approximation signal of a healthy and a broken bar machine.

In [22], the decomposition level n has been chosen in order to obtain an approximation signal and two details with frequency bands below f_{net} . Like in [21], a wavelet with good filtering properties is needed (e.g., a DB40 wavelet). The decomposition level n depends on the sampling rate f_s and on the frequency net f_{net} . It can be calculated using the following formula:

$$n > \frac{\log(f_s/f_{net})}{\log(2)} + 1 \quad (10)$$

e.g., for $f_s = 5000$ Hz and $f_{net} = 50$ Hz $n = 8$. In Fig. 5 we can see the results when analyzing a broken bar SCIM startup current. In Fig. 6 we can see the same DWT decomposition (more precisely, the A8, D8 and D7 signals), for the case of a healthy SCIM startup current. The SCIM has a broken bar if we find the characteristic time – frequency evolution pattern of the LSH reflected on the approximation signal and the first two detail

signals.

The diagnosis method presented in [23], extracts the FC of a stator SC and applies the DWT to the remaining signal in order to detect the LSH presence. The extraction algorithm is based on a least squares error criterion. The DWT is applied to the remaining signal in order to obtain the 9 decomposition level detail coefficients (note the difference between the detail coefficients and the detail signal: the detail signal is reconstructed summing the wavelets sons weighted by their respective detail coefficients). If the SCIM diagnosed has any broken bar, the presence of the LSH in the SC increases the energy of the SC on some regions of the time – frequency plane, producing an increment of certain 9 detail DWT coefficients. In order to detect the bar breakage automatically [24], the square of the coefficients that increase when the SCIM has a broken bar are summed. If the factor obtained reaches a certain level, the diagnosis system indicates a bar breakage.

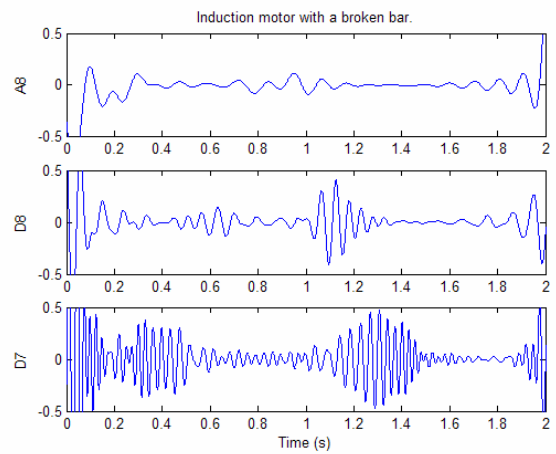


Fig. 5 Level 8 DWT decomposition of a broken bar SCIM startup current.

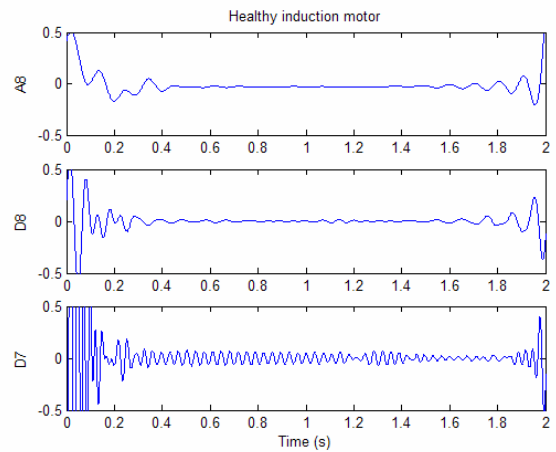


Fig. 6 Level 8 DWT decomposition of a healthy SCIM startup current.

Other works use the DWT to analyze the stator current during steady state. For example, Cusidó et al. prove in [25] that the DWT can be applied to the “steady state” stator current of a SCIM in order to detect broken rotor bars and stator short circuits, even if a variation on the load torque occurs. If we can measure or estimate the rotor speed during the test, we can calculate the evolution of the LSH frequency. The DWT is applied conveniently in order to obtain a detail signal containing the frequency band that the LSH has covered during the test. Finally,

the energy of that signal is calculated. If it is high, then the SCIM has a broken bar.

4. Conclusions.

The analysis of the SC for the detection of broken bars solves the drawbacks of the analysis of the steady state current. It also has important advantages:

- Regardless of the load conditions, the amplitudes of the SH during the startup, reach values several times higher than those in steady state. As a result of that, the proofs of the bar breakage are much more evident.
- Moreover, when the slip changes during the startup, the SH frequencies change, leading to a unique time-frequency evolution pattern of the LSH and USH harmonics. The detection of that evolution helps to discard non-fault related harmonics like those generated by periodic loads or voltage unbalances.

The Wavelet Transform can be used to analyze the SC of the SCIM being diagnosed in order to detect bar breakages. Any of the four general approaches explained can be followed.

The main problem of the CWT is that it consumes a lot of computational time. On the other hand, when it is well used, it can give an excellent view of the SH frequencies evolution. The DWT can be computed very quickly. Moreover, the SC can be easily reconstructed as a sum of the approximation signal and the details.

Examples of those main approaches have been given, with the specific solutions proposed by their authors. Through the revision, the Wavelet Transform has proved to be an excellent mathematical tool for the detection of broken bars.

Acknowledgments

This work was supported by the European Community's Seventh Framework Program FP7/2007-2013 under Grant Agreement 224233 (Research Project PRODI "Power plant Robustification based on fault Detection and Isolation algorithms").

References

- [1] A. Bellini, F. Filippetti, G. Franceschini, C. Tassoni, and G. B. Kliman, "Quantitative evaluation of induction motor broken bars by means of electrical signature analysis," *IEEE Transactions on Industry Applications*, vol. 37, no. 5, pp. 1248–1255, Sep./Oct. 2001.
- [2] S. Nandi and H. A. Toliyat, "Condition monitoring and fault diagnosis of electrical motors—A review," *IEEE Trans. Energy Convers.*, vol. 20, no. 4, pp. 719–729, Dec. 2005.
- [3] G. B. Kliman, R. A. Koegl, J. Stein, R. D. Endicott, and M. W. Madden, "Noninvasive detection of broken rotor bars in operating induction motors," *IEEE Trans. Energy Convers.*, vol. 3, no. 4, pp. 873–879, Dec. 1988.
- [4] N.M. Elkasabgy, A. R. Eastham, and G. E. Dawson, "Detection of broken rotor bars in the cage rotor on an induction machine," *IEEE Trans. Ind. Appl.*, vol. 28, no. 1, pp. 165–171, Jan./Feb. 1992.
- [5] M. Eltabach, A. Charara, and I. Zein, "A comparison of external and internal methods of signal spectral analysis for broken rotor bars detection in induction motors," *IEEE Trans. Ind. Electron.*, vol. 51, no. 1, pp. 107–121, Feb. 2004.
- [6] A. M. Trzynadlowski and E. Ritchie, "Comparative investigation of diagnostic media for induction motors: A case of rotor cage faults," *IEEE Trans. Ind. Electron.*, vol. 47, no. 5, pp. 1092–1099, Oct. 2000.
- [7] W. T. Thomson and M. Fenger, "Current signature analysis to detect induction motor faults," *IEEE Ind. Appl. Mag.*, vol. 7, no. 4, pp. 26–34, Jul./Aug. 2001.
- [8] R. R. Schoen and T. G. Habetler, "Evaluation and implementation of a system to eliminate arbitrary load effects in current-based monitoring of induction machines," *IEEE Trans. Ind. Appl.*, vol. 33, no. 6, pp. 1571–1577, Nov./Dec. 1997.
- [9] M. C. Ian and R. Wendell, "Using current signature analysis technology to reliably detect cage winding defects in squirrel-cage induction motors," *IEEE Trans. Ind. Appl.*, vol. 43, no. 2, pp. 422–428, Mar./Apr. 2007.
- [10] A. Bellini, F. Filippetti, G. Franceschini, C. Tassoni, R. Passaglia, M. Saottini, G. Tontini, M. Giovannini, and A. Rossi, "On-field experience with online diagnosis of large induction motors cage failures using MCSA," *IEEE Trans. Ind. Appl.*, vol. 38, no. 4, pp. 1045–1053, Jul./Aug. 2002.
- [11] J. F. Watson and S. Elder, "Transient analysis of the line current as a fault detection technique for 3-phase induction motors," in *Proc. ICEM*, Manchester, U.K., Sep. 1992, pp. 1241–1245.
- [12] R. Puche-Panadero, M. Pineda-Sanchez, M. Riera-Guasp, J. Roger-Folch, E. Hurtado-Perez, and J. Perez-Cruz, "Improved resolution of the MCSA method via Hilbert Transform, enabling the diagnosis of rotor asymmetries at very low slip," *IEEE Transaction on Energy Conversion*, Vol. 24, No 1, pp. 52-59, 2009.
- [13] F. Filippetti, G. Franceschini, C. Tassoni, and P. Vas, "AI techniques in induction machines diagnosis including the speed ripple effect," *IEEE Trans. Ind. Appl.*, vol. 34, no. 1, pp. 98–108, Jan./Feb. 1998.
- [14] R. R. Schoen and T. G. Habetler, "Evaluation and implementation of a system to eliminate arbitrary load effects in current-based monitoring of induction machines," *IEEE Trans. Ind. Appl.*, vol. 33, no. 6, pp. 1571–1577, Nov./Dec. 1997.
- [15] M. Riera-Guasp, J.A. Antonino-Daviu, J. Roger-Folch and M.P. Molina-Palomares, "The use of the wavelet approximation signal as a tool for the diagnosis of rotor bar failures", *IEEE Transactions on Industry Applications*, vol. 44, pp. 716-726, 2008.
- [16] I. Daubechies, "Ten Lectures on Wavelets". Philadelphia, PA: SIAM, 1992.
- [17] S.G. Mallat, "A wavelet tour of signal processing". San Diego: Academic Press, 1998.
- [18] R. Supangat, N. Ertugrul, W. L. Soong, D. A. Gray, C. Hansen, and J. Grieger, "Detection of broken rotor bars in induction motor using starting-current analysis and effects of loading," *IEE Proceedings Electric Power Applications*, vol. 153, pp. 848-855, 2006.
- [19] Z. Zhengping, R. Zhen, and H. Wenying, "A novel detection method of motor broken rotor bars based on wavelet ridge," *IEEE Transactions on Energy Conversion*, vol. 18, pp. 417-423, 2003.
- [20] F. Briz, M. W. Degner, P. Garcia, and D. Bragado, "Broken Rotor Bar Detection in Line-Fed Induction Machines Using Complex Wavelet Analysis of Startup Transients," *IEEE Transactions on Industry Applications*, vol. 44, pp. 760-768, 2008.
- [21] J. Antonino-Daviu, M. Riera-Guasp, J. Roger-Folch, F. Martínez-Giménez, and A. Peris, "Application and optimization of the discrete wavelet transform for the detection of broken rotor bars in induction machines," *Applied and Computational Harmonic Analysis*, vol. 21, pp. 268-279, 2006.
- [22] J. A. Antonino-Daviu, M. Riera-Guasp, J. R. Folch, and M. Pilar Molina Palomares, "Validation of a new method for the diagnosis of rotor bar failures via wavelet transform in industrial induction machines," *IEEE Transactions on Industry Applications*, vol. 42, pp. 990-996, 2006.
- [23] H. Douglas, P. Pillay, and A. K. Ziarani, "Broken rotor bar detection in induction machines with transient operating speeds," *IEEE Transactions on Energy Conversion*, vol. 20, pp. 135-141, 2005.
- [24] A. Ordaz-Moreno, R. de Jesus Romero-Troncoso, J. A. Vite-Frias, J. R. Rivera-Gillen, and A. Garcia-Perez, "Automatic Online Diagnosis Algorithm for Broken-Bar Detection on Induction Motors Based on Discrete Wavelet Transform for FPGA Implementation," *IEEE Transactions on Industrial Electronics*, vol. 55, pp. 2193-2202, 2008.
- [25] J. Cusido, L. Romeral, J. A. Ortega, J. A. Rosero, and A. Garcia Espinosa, "Fault Detection in Induction Machines Using Power Spectral Density in Wavelet Decomposition," *IEEE Transactions on Industrial Electronics*, vol. 55, pp. 633-643, 2008.